

# Finite-rate quenches of site bias in the Bose-Hubbard dimer

T. Venumadhav,<sup>1,2</sup> Masudul Haque,<sup>1</sup> and R. Moessner<sup>1</sup>

<sup>1</sup>Max-Planck Institute for the Physics of Complex Systems, Nöthnitzer Str. 38, 01187 Dresden, Germany

<sup>2</sup>Department of Physics, Indian Institute of Technology, Kanpur 208016, India

(Received 20 January 2010; published 16 February 2010)

For a Bose-Hubbard dimer, we study quenches of the site energy imbalance, taking a highly asymmetric Hamiltonian to a fully symmetric one. The ramp is carried out over a finite time that interpolates between the instantaneous and adiabatic limits. We provide results for the excess energy of the final state compared to the ground-state energy of the final Hamiltonian as a function of the quench rate. This excess energy serves as the analog of the defect density that is considered in the Kibble-Zurek picture of ramps across phase transitions. We also examine the fate of quantum “self-trapping” when the ramp is not instantaneous.

DOI: [10.1103/PhysRevB.81.054305](https://doi.org/10.1103/PhysRevB.81.054305)

PACS number(s): 67.85.Hj, 03.75.Lm, 05.30.Jp, 64.70.Tg

## I. INTRODUCTION

Explicit time evolution of quantum many-particle systems out of equilibrium has generated intense interest due to unprecedented possibilities for experimentally accessible non-equilibrium situations opened up by developments in laser-cooled atomic clouds and in mesoscopic systems. One theme has been the response to an instantaneous “quench,” where a physical parameter is suddenly changed to a different value. While instantaneous quenches are more convenient to analyze, a change in parameter can of course be performed at any rate. At the other extreme from the instantaneous quench, one can make the parameter sweep *adiabatically*, in which case the system reaches the ground state of the final Hamiltonian. The Kibble-Zurek theory describes finite-rate ramps, neither instantaneous nor adiabatic, across phase transitions.<sup>1</sup> While the original interest concerned thermal phase transitions, there has been a recent surge of interest in finite-rate traversals of *quantum* phase transitions in lattice Hamiltonians (Refs. 2–4 and references therein). One important context is the Bose-Hubbard Hamiltonian, where finite-rate ramps of the Hubbard interaction  $U$  have been analyzed,<sup>4–6</sup> motivated by an influential experiment quenching across the Mott-superfluid transition.<sup>7</sup>

In this work, we analyze finite-rate ramps in a Bose-Hubbard dimer. For far-from-equilibrium issues where few standard theoretical techniques exist, it is of obvious interest to look at finite clusters because of near-exact solvability. One can hope to understand the nonequilibrium dynamics in some detail. Such detailed results for clusters clearly provide an invaluable background for the emerging field of nonequilibrium dynamics in macroscopic (many-site) quantum systems. In addition, the bosonic dimer is an important model system by itself, and its physics is relevant in diverse contexts. In recent years several experiments have achieved two-site bosonic systems in cold-atom setups.<sup>8–12</sup> The quenches we study could be implemented in such a setup, e.g., through slower ramps in the experiment of Ref. 8. The Bose-Hubbard dimer can be mapped onto a single-spin Hamiltonian,<sup>13–19</sup> very similar to that governing single-molecule magnetic experiments, where finite-rate ramps have received some attention.<sup>20,21</sup> Finite-rate quenches have also been reported with a Josephson junction arrangement,<sup>22</sup> which is closely related to a bosonic dimer.

For  $N$  bosons in two sites, the Hamiltonian is

$$H = -\frac{K}{2}(a_1^\dagger a_2 + a_2^\dagger a_1) + \frac{U}{2} \sum_{i=1}^2 n_i(n_i - 1) + \frac{\delta}{2}(n_1 - n_2),$$

with  $n_i = a_i^\dagger a_i$  and  $\langle n_1 \rangle + \langle n_2 \rangle = N$ .

Quenches of the interaction  $U$  in the dimer have been considered in Refs. 4–6 and 23. However, for the dimer, quenches of the site bias parameter  $\delta$  are also of natural interest. Instantaneous quenches of  $\delta$  from an imbalanced to a symmetric situation, i.e.,  $\delta(t) = \delta_0 \theta(-t)$ , have been studied as a quantum realization of self-trapping.<sup>13–19</sup> Classical self-trapping, described by the two-mode Gross-Pitaevskii equation, is the persistence of imbalance in the state despite the final Hamiltonian being unbiased.<sup>8,24</sup> In the quantum case, the relative number imbalance  $z = \langle n_1 - n_2 \rangle / N$  oscillates after the instantaneous quench, with decay and long-time revivals of the oscillations. For small  $\delta_0$ , the imbalance oscillations are around zero. However, for large enough values of  $\delta_0$  and  $NU/K$ , after a fast quench the mean value of the oscillating  $z(t)$  does not relax to zero within any reasonable time scale.<sup>13–19</sup> The astronomically long relaxation times (“quantum self-trapping”) can be understood in terms of extremely small energy splittings in the eigenvalue spectrum of the final Hamiltonian. For the instantaneous quench, the various relationships between time scales of dynamical features and energy scales of the  $\delta=0$  spectrum has been discussed in some detail in the literature.<sup>13–19</sup>

We use  $U=1$ , measuring energy (time) in units of  $U[\hbar/U]$ . We focus mostly on the regime  $K \ll U$ . We will analyze finite-rate quenches of  $\delta$  of the form

$$\delta(t) = -\delta_0 \theta(-t) + (-\delta_0/\tau)(\tau-t)\theta(t)\theta(\tau-t),$$

as illustrated in Figs. 1(a) and 1(b). We consider the whole range from  $\tau=0$  (instantaneous) to  $\tau \rightarrow \infty$  (adiabatic). The initial ( $t=0$ ) state is taken to be the ground state of the initial Hamiltonian with  $\delta=-\delta_0$ . The initial asymmetry  $\delta_0$  is taken to be large enough that the bosons are initially concentrated almost entirely on site 1, i.e., the wave function is dominated by  $|N, 0\rangle$ . The final ground state is dominated by  $|N/2, N/2\rangle$  but the system does not reach this ground state unless the quench is truly adiabatic. Figure 1(c) demonstrates how

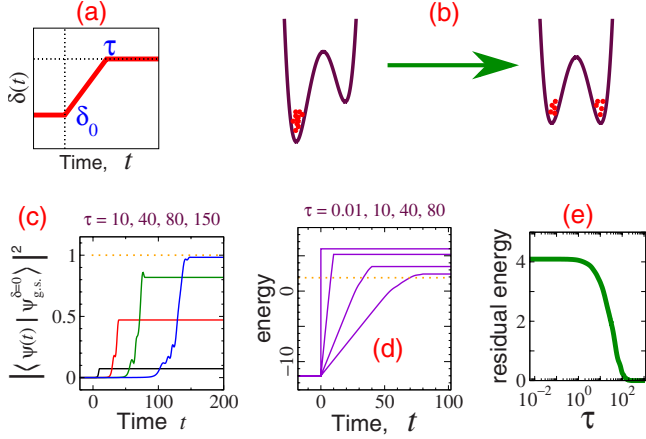


FIG. 1. (Color online) [(a) and (b)] Form of quench analyzed in this work. Lower panels illustrate the approach to adiabaticity with increasing  $\tau$  for  $(N, K, \delta_0) = (4, 0.2, 9)$ . (c) Overlap with ground state of final Hamiltonian. Curves from lowest to highest final values correspond to  $\tau = 10, 40, 80, 150$ . (d) Evolution of energy: curves from top to bottom are  $\tau = 0.01, 10, 40, 80$ . Dotted horizontal line is the ground-state energy of the final Hamiltonian. The final excess energy over this dotted line is the residual energy, which decreases with  $\tau$  (e). Energy and time are measured in units of  $U$  and  $\hbar/U$ , respectively.

larger- $\tau$  quenches are more nearly adiabatic, through the temporal evolution of overlaps with the  $\delta=0$  ground state.

In Kibble-Zurek theory, one uses the *defect density* in the final ordered state to quantify the deviation from adiabaticity. In few-site clusters, defects are not easily defined nor are phase transitions or ordering. However, there is a natural quantity that serves an analogous role, namely, the final energy after the quench,  $E_{t>\tau} = \langle \psi_{t>\tau} | H^{\delta=0} | \psi_{t>\tau} \rangle$ . In an adiabatic sweep, the final energy is the ground-state energy  $E_{g.s.}^{\delta=0}$  of the final Hamiltonian. The excess energy over  $E_{g.s.}^{\delta=0}$  (*residual energy*) measures the deviation from adiabaticity.<sup>3</sup> The interpolation between instantaneous and adiabatic limits is illustrated through energy evolution in Fig. 1(d) and through residual energies in Fig. 1(e).

Our main results concern the dependence of the residual energy,  $\Delta E = E_{t>\tau} - E_{g.s.}^{\delta=0}$ , on the quench time  $\tau$ . For near-instantaneous quenches (small  $\tau$ ), the energy deviation from the instantaneous limit is found to scale as  $\tau^2$ . We analyze larger- $\tau$  quenches through a multicrossing Landau-Zener<sup>25</sup> scenario and derive concise expressions for  $\Delta E$  in an intermediate- $\tau$  regime as well as in the near-adiabatic (very large  $\tau$ ) limit.

While we focus on  $\Delta E$ , our analysis can in principle be adapted to treat other observables. Since instantaneous  $\delta$  quenches are associated with the self-trapping phenomenon, we also ask whether and how self-trapping survives when the ramp rate is finite.

## II. SLOW QUENCHES

Our analysis for large  $\tau$  relies on the avoided level crossing structure of the problem. Figures 2(a)–2(c) shows that the level crossing structure is only relevant for small  $K$ . Our

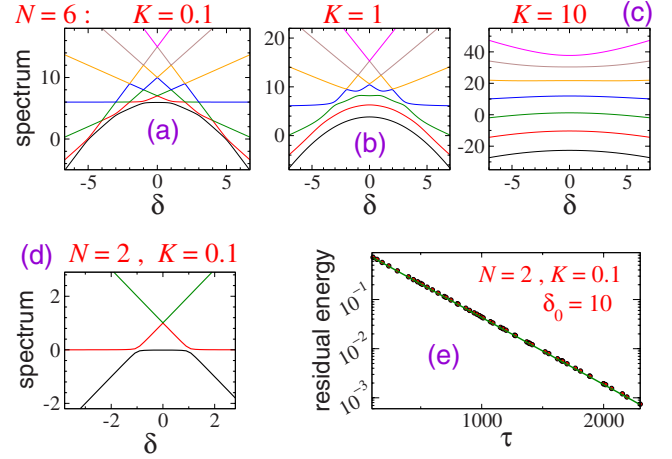


FIG. 2. (Color online) [(a)–(c)] energy spectra for  $N=6$  bosons. For small  $K$  and even  $N$ , the lowest state goes through  $N/2$  avoided level crossings on either side of  $\delta=0$ , at  $\delta = \pm(2x-1)U$ , with  $x=1, 2, \dots, N/2$ . (d)  $N=2$  bosons. (e) Residual energy; dots are exact values and line is theory. Energy and time are measured in units of  $U$  and  $\hbar/U$ , respectively.

analytic treatment for slow quenches is focused on this parameter region,  $K \ll U$  [Fig. 2(a)]. Therefore, we can regard the quench problem as one of traversing a sequence of well-separated avoided level crossings. This scenario would clearly not be applicable for situations such as those in Figs. 2(b) and 2(c).

We start with the simplest case of two bosons. There is only one level crossing encountered during the quench, at  $\delta \approx -1$ , where the  $|2, 0\rangle$  and  $|1, 1\rangle$  states are mixed [Fig. 2(d)]. The Hamiltonian within this space is  $H = \begin{pmatrix} 1+\delta(t) & -K/\sqrt{2} \\ -K/\sqrt{2} & 0 \end{pmatrix}$ . The Landau-Zener formula<sup>25</sup> gives the probability of excitation at this level crossing to be  $p = e^{-2\pi\gamma}$ , where  $\gamma = (K/\sqrt{2})^2 / \dot{\delta}$ . At the end of the quench, the energy has a contribution of weight  $(1-p)$  from the ground state (energy  $\approx 0$ ) and a contribution of weight  $p$  from the two higher levels (energy  $\approx U$ ). Thus the residual energy is  $\Delta E \approx U e^{-(\pi K^2/\delta_0)\tau}$ . This reproduces numerical calculations for large  $\tau$  [Fig. 2(e)].

For larger numbers of bosons, the quantum state can take various paths to  $\delta=0$ , in a multicrossing situation such as that shown in Fig. 2(a). Fortunately, at small  $K$  the higher crossings are simple to treat because the energy splitting at these points are of higher than linear order in  $K$ . Thus for  $K \ll U$  one can regard these as real crossings rather than avoided crossings so that the excitation probabilities are unity. One therefore has to consider only the excitation probabilities at the  $N/2$  crossings involving the lowest energy state. The excitation probabilities are

$$p_i = \exp \left[ -\frac{\pi}{2} i(N-i+1) K^2 \tau / \delta_0 \right]$$

at the  $i$ th crossing encountered during the quench; here  $i(N-i+1)$  is the bosonic factor relevant for the coupling between states  $|N-i+1, i-1\rangle$  and  $|N-i, i\rangle$ . Any weight going into the upper level at the  $(\frac{N}{2} - \alpha + 1)$ th crossing goes straight

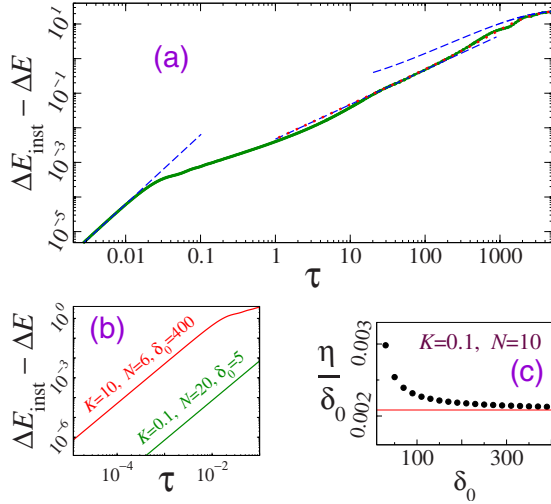


FIG. 3. (Color online) (a)  $(N, K, \delta_0) = (10, 0.1, 300)$ . Thick line: exact numerical values. The three dashed lines are the analytical results for small, intermediate, and large  $\tau$  [Eqs. (5), (2), and (3)]. Equation (1) is dotted line interpolating between 2 and 3 but is barely visible because the exact curve almost coincides. (The exact curve has some additional oscillations.) (b) Quadratic behavior, shown here for cases we do not treat analytically, large  $K$  (upper) and  $\delta_0 < NU$  (lower). (c) Coefficient  $\eta$  follows Eq. (5) (horizontal line) when  $\delta_0 \gg NU$ . Energy and time are measured in units of  $U$  and  $\hbar/U$ , respectively.

on to the final energy  $E_\alpha$  since we neglect further deflection at the higher crossings. The final ( $\delta=0$ ) energies are  $E_\alpha \approx \frac{N(N-2)}{4} + \alpha^2$ , with  $\alpha=0, 1, \dots, N/2$ . From this picture, the final energy is found to be

$$p_1 E_{N/2} + (1-p_1)p_2 E_{N/2-1} + (1-p_1)(1-p_2)p_3 E_{N/2-2} + \dots + \left[ \prod_{i=1}^{N/2-1} (1-p_i) \right] p_{N/2} E_1 + \left[ \prod_{i=1}^{N/2} (1-p_i) \right] E_0. \quad (1)$$

For moderate values of  $N$  for which exact numerical evolution is feasible up to large times, we find this relationship to work very well at small  $K$  [e.g., Fig. 3(a)].

There are two situations, corresponding to distinct physical pictures of the excitation process, where Eq. (1) reduces to compact forms. First, when  $\tau$  is large enough that one can use the Landau-Zener formula but small enough that the  $p_i = e^{-a_i \tau}$  are close to unity, the excitation at the first two crossings deplete the weight since  $p_{1,2} \approx 1$ . Thus only the top two final levels ( $E_{N/2}$  and  $E_{N/2-1}$ ) contribute to the final energy. Expanding  $p_1 = e^{-a_1 \tau}$  to linear order, one gets for this intermediate regime

$$\Delta E_{\text{inst.}} - \Delta E \approx (N-1) \frac{\pi K^2 N}{2 \delta_0} \tau. \quad (2)$$

Here  $\Delta E_{\text{inst.}}$  is the residual energy for the instantaneous case ( $\tau=0$ ), namely,  $\langle \psi_{t=0} | H^{\delta=0} | \psi_{t=0} \rangle - E_{g.s.}^{\delta=0}$ . We have used  $\Delta E_{\text{inst.}} \approx E_{N/2} - E_0 \approx N^2/4$ . (In an instantaneous quench, the weight would all go to the highest final level.) One could also extend the above analysis by including the third crossing and expanding up to  $\tau^2$ . Obviously, including further levels

and expanding the exponentials up to higher orders in  $\tau$ , one eventually gets back the full expression (1). Note that, although we have obtained a linear intermediate behavior in  $\tau$ , this is a nonperturbative result since it is based on Landau-Zener probabilities.

Second, at very large  $\tau$  the  $p_i$  are small so that  $p_1 \ll p_2 \ll \dots \ll p_{N/2}$  because of the bosonic factors  $i(N-i+1)$ . Neglecting  $p_{i>1}$ , one obtains

$$\Delta E \approx p_1 E_{N/2} - p_1 E_0 \approx \frac{1}{4} N^2 \exp \left[ -\frac{\pi N K^2}{2 \delta_0} \tau \right]. \quad (3)$$

Only the lowest and highest energy levels contribute in this case.

Figure 3(a) shows an example where the behaviors of Eqs. (1)–(3) can be seen in exact numerical calculations. The small oscillations at large  $\tau$  on top of Eqs. (1) and (3) are interference effects, discussed later.

### III. FAST QUENCHES

We now consider small  $\tau$ , i.e., almost instantaneous quenches. The main observation is that the residual energy has the dependence

$$\Delta E = \Delta E_{\text{inst.}} - \eta \tau^2 + \mathcal{O}(\tau^\gamma), \quad (\gamma > 2). \quad (4)$$

The quadratic behavior is very robust and is present for all values of  $N$ ,  $\delta_0$ , and  $K$  we have checked [Fig. 3(a) and 3(b)]. In Fig. 3(a), we can see the quadratic behavior (straight line in log-log plot) for a  $K \ll NU \ll \delta_0$  case, which is the parameter region we analyze. Figure 3(b) shows quadratic behaviors for cases outside this parameter regime.

To explain this behavior, we start with  $N=2$  bosons. Writing the wave function as  $|\psi(t)\rangle = c_1(t)|2,0\rangle + c_2(t)|1,1\rangle + c_3(t)|0,2\rangle$ , one can consider equations of motion for  $c_i$ , e.g.,  $\dot{c}_1(t) = -i[U - \delta(t)]c_1(t) + i\frac{K}{\sqrt{2}}c_2(t)$ , and solve for small orders in time:

$$c_i(t) = c_i(0) + \dot{c}_i(0)t + \frac{1}{2}\ddot{c}_i(0)t^2 + \mathcal{O}(t^3).$$

Since  $\dot{c}_i(0)$  is entirely imaginary, the linear terms in  $t$  are imaginary. Linear- $t$  terms will thus cancel out from observable quantities like  $|c_i(t)|^2$  and  $c_1(t)^*c_1(t) + c_1(t)c_1(t)^*$ , which appear in the expression for the final energy:  $U(|c_1|^2 + |c_3|^2) - \frac{K}{\sqrt{2}}[c_1^*c_2 + c_2^*c_3 + \text{H.c.}]$ . The energy at  $\tau$  thus has a constant and a  $\tau^2$  term but no  $\mathcal{O}(\tau)$  term.

For  $N=2$ , we can express the coefficient  $\eta$  in Eq. (4) analytically in terms of the initial  $c_i(t=0)$  and also write analytic expressions for  $c_i(0)$  as solutions of cubic polynomials. Unfortunately, these expressions are too cumbersome to be useful. For  $\delta_0 \gg U, K$ , one can calculate perturbatively, yielding  $\eta \sim K^2 \delta_0 / 24$ .

For  $N>2$ , the same argument holds for a leading  $\tau^2$  correction. For very large  $\delta_0$  and small enough  $\tau$ , one can use the approximation that only the most imbalanced configurations are excited and restrict to the subspace  $|N,0\rangle$ ,  $|N-1,1\rangle$ , and  $|N-2,2\rangle$ . The calculation is then similar to the  $N=2$  case. One obtains

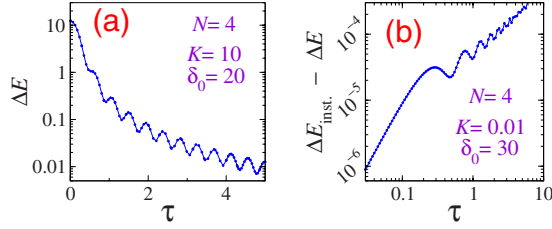


FIG. 4. (Color online) (a) Quantum interference at large  $K$ . (b) Interferences resulting from using  $|N,0\rangle$  as initial state. Energy and time are measured in units of  $U$  and  $\hbar/U$ , respectively.

$$\eta \sim \frac{NK^2\delta_0}{48}, \quad \Delta E \sim \Delta E_{\text{inst.}} - \frac{NK^2\delta_0}{48}\tau^2, \quad (5)$$

at leading order in  $\delta_0^{-1}$ . This also contains the  $N=2$  result. Figures 3(a) and 3(c) show that this expression works well for  $\delta_0 \gg NU \gg K$ .

While this compact result is valid only for  $\delta_0 \gg NU \gg K$ , the level crossing structure plays no role in this analysis, so in principle it can be applied also to other parameter regimes; however the expressions for  $\eta$  are too complicated to be useful in such cases.

Figure 3(a) also displays the entire instantaneous-to-adiabatic crossover, which includes our slow-quench and fast-quench results but also a range of  $\tau$  ( $\sim 0.02$  to  $\sim 20$ ) for which we do not have simple descriptions.

#### IV. QUANTUM INTERFERENCES

Our treatment of multicrossing configurations (Fig. 2) utilized unit excitation probabilities at the higher crossings, which is valid at small  $K$ . However, if there is substantial splitting at each crossing, the configurations offer rich possibilities for quantum interference of different paths. We have already seen interference signatures in the mild oscillatory behavior in Fig. 3(a) for  $(N,K)=(10,0.1)$  in the near-adiabatic regime. In Fig. 4(a) we show more pronounced interference effects at large  $K$ .

Interference between paths also becomes prominent when the initial state is not the ground state but has weights in more than one eigenstate, e.g., if one starts with the state  $|N,0\rangle$  [Fig. 4(b)]. This is not exactly the ground state at  $\delta=-\delta_0$  as long as  $\delta_0$  is finite. It could however easily be an experimentally relevant initial state.

#### V. SELF-TRAPPING WITH FINITE-RATE QUENCHES

We now consider the effect of finite quench times on the quantum self-trapping phenomenon.<sup>13–19</sup> Self-trapping involves dynamics starting with a biased state, which is the case for an instantaneous  $\tau=0$  quench from large negative  $\delta=-\delta_0$ . This is the type of dynamics analyzed in Ref. 13. The relative number imbalance  $z=\langle n_1-n_2 \rangle/N$  can oscillate around a nonzero value of  $z$  if  $NU/K$  and the starting  $z$  are large enough. Since the state  $\psi_{t=\tau}$  after a finite- $\tau$  quench is closer to the unbiased ( $z=0$ ) ground state at  $\delta=0$ , self-trapping is clearly weakened at larger  $\tau$ .

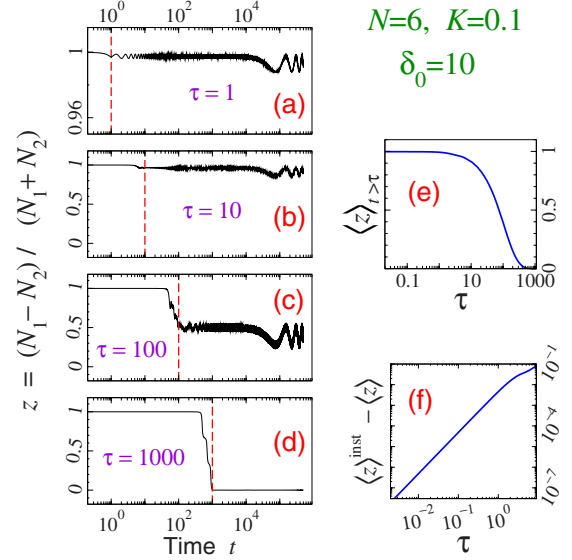


FIG. 5. (Color online) Fate of self-trapping. [(a)–(d)] Number imbalance dynamics during and after quench for various quench times. Note different scale on top panel a. (e) Long-time average of relative number imbalance after quench is over at  $t=\tau$ . Averaging is performed between  $t=\tau$  and  $t=t_{\text{up}}=500000$ . (f) Quadratic deviation of  $\langle z \rangle_{t>\tau}$  from instantaneous case for small  $\tau$ . Time is measured in units of  $\hbar/U$ .

We can characterize self-trapping through the long-time average of  $z=\langle n_1-n_2 \rangle/N$  at times  $t>\tau$ . A nonzero  $\langle z \rangle_{t>\tau}$  indicates self-trapping. The definition is somewhat subtle because quantum self-trapping involves nonzero  $\langle z \rangle_{t>\tau}$  up to some very large time but not really infinite times. [This very large time scale is due to the tiny splitting energies of the higher level crossings in Fig. 2(a).<sup>13–19</sup>] The long-time average therefore depends on the upper time limit  $t_{\text{up}}$  up to which  $z(t)$  is averaged and will always be zero for large enough  $t_{\text{up}}$ . This is in contrast to the classical self-trapping observed in the two-site discrete nonlinear Schrödinger equation, where the self-trapped states are truly stationary states.<sup>24</sup>

In Figs. 5(a)–5(d) we demonstrate the weakening of the self-trapping effect at larger  $\tau$ , through the behavior of  $z(t)$ . The logarithmic scale highlights the fact that there are several important time scales in the dynamics. The intermediate- $\tau$  cases have more complicated wave functions at the end of the quench as analyzed in Sec. II. Hence the dynamics is most interesting for intermediate  $\tau$ . This can be seen for example through a larger number of peaks in the Fourier transform of the intermediate- $\tau$  time evolution data. In comparison, the  $\tau \lesssim 1$  and  $\tau \gg 100$  cases show fewer high-frequency components in the dynamics.

Figure 5(e) shows the dependence of  $\langle z \rangle_{\tau < t < t_{\text{up}}}$  on  $\tau$ . The averaging displayed in Figs. 5(e) and 5(f) was performed up to  $t_{\text{up}}=5 \times 10^5$ ; the  $z(t)$  behaviors in Figs. 5(a)–5(d) suggests this is a reasonable value for capturing the self-trapping phenomenon. The behavior of  $\langle z \rangle$  is similar to the  $\tau$  dependence of the residual energy  $\Delta E$  [Fig. 1(e)]; however the ambiguity in the averaging procedure makes it difficult to perform a systematic analysis similar to what we have presented for  $\Delta E$  in previous sections. The similarity of Figs. 1(e) and 5(e) is not surprising because both the  $z(t>\tau)$  dynamics and the



final energy are determined by the state at the end of the quench, i.e., the weight of excited states in  $\psi_{t=\tau}$ . At small  $\tau$  there is also a quadratic deviation of  $\langle z \rangle_{t>\tau}$  from the instantaneous case [Fig. 5(f)] as there is for  $\Delta E$ .

## VI. SUMMARY AND OPEN ISSUES

This work analyzes finite-rate quenches most relevant to the self-trapping phenomenon, namely, from  $\delta = -\delta_0$  to  $\delta = 0$  with parameters  $K \ll NU \ll \delta_0$ . While quenches of the tilt  $\delta$  are natural for the dimer, it is relatively new in the nonequilibrium literature because bias quenches do not appear naturally in the many-site case. We provide concise analytical results for the residual energy in parametrically different regimes of small, intermediate, and large  $\tau$  [Eqs. (5), (2), and (3)]. The small  $\tau$  result (5) is perturbative in  $\tau$ , while Eqs. (2) and (3) are obtained from the Landau-Zener formula and are thus nonperturbative, despite the linear dependence [Eq. (2)] at intermediate  $\tau$ .

The importance of Bose-Hubbard dimer dynamics reaches far beyond the cold-atom context, as the model appears in diverse areas of physics. For example, it is equivalent to a large-spin Hamiltonian:  $H = -KJ_x + UJ_z^2 + \delta J_z$ . This describes single-molecule magnets. However for molecular magnet experiments the anisotropy ( $J_z^2$ ) term usually has negative co-

efficient and effects of host lattice vibrations or nuclear spins cannot always be neglected.

The residual energy is in principle experimentally measurable in cold-atom realizations through time-of-flight measurements that provide energy information from the cloud expansion rate (e.g., Ref. 26). For molecular magnet experiments energy is difficult to measure, but magnetization dynamics [analogous to our  $z(t)$  dynamics] is commonly reported.

Our work raises a number of open issues. There are a number of parameter regimes other than ours which might be of interest. Examples are other values of initial and final  $\delta$  or of  $K/U$ . References 27 and 28 have considered sweeps of  $\delta$  from negative to positive infinity for parameter regions and initial states quite different from ours. Clearly, we are only seeing the beginning stages of an emerging unified dynamical picture. Another intriguing issue is the connection to the mean-field description via the discrete Gross-Pitaevskii equation. Reference 28 has worked out some Landau-Zener issues for the mean-field dimer, for  $U < 0$  and  $(-\infty \rightarrow +\infty)$  sweeps. Numerical explorations for  $(-\delta_0 \rightarrow 0)$  quenches have shown us behaviors similar to what we have presented for the full quantum case. Finally, the present results may need to be adapted for specific realizations, once such experiments are designed.

<sup>1</sup>T. W. B. Kibble, J. Phys. A **9**, 1387 (1976); Phys. Rep. **67**, 183 (1980); W. H. Zurek, Nature (London) **317**, 505 (1985); Phys. Rep. **276**, 177 (1996).

<sup>2</sup>For recent work, see, e.g., K. Sengupta and D. Sen, Phys. Rev. A **80**, 032304 (2009); S. Miyashita, H. De Raedt, and B. Barbara, Phys. Rev. B **79**, 104422 (2009); F. Pollmann, S. Mukerjee, A. G. Green, and J. E. Moore, Phys. Rev. E **81**, 020101 (2010); D. Patanè, L. Amico, A. Silva, R. Fazio, and G. E. Santoro, Phys. Rev. Lett. **101**, 175701 (2008); U. Divakaran and A. Dutta, Phys. Rev. B **79**, 224408 (2009); S. Mondal, K. Sengupta, and D. Sen, *ibid.* **79**, 045128 (2009); L. Cincio, J. Dziarmaga, J. Meisner, and M. M. Rams, *ibid.* **79**, 094421 (2009); S. Mondal, D. Sen, and K. Sengupta, *ibid.* **78**, 045101 (2008); R. Schützhold, J. Low Temp. Phys. **153**, 228 (2008); R. Barankov and A. Polkovnikov, Phys. Rev. Lett. **101**, 076801 (2008); D. Sen, K. Sengupta, and S. Mondal, *ibid.* **101**, 016806 (2008); K. Sengupta, D. Sen, and S. Mondal, *ibid.* **100**, 077204 (2008); V. Mukherjee, U. Divakaran, A. Dutta, and D. Sen, Phys. Rev. B **76**, 174303 (2007); M. Uhlmann, R. Schützhold, and U. R. Fischer, Phys. Rev. Lett. **99**, 120407 (2007); A. Das, K. Sengupta, D. Sen, and B. K. Chakrabarti, Phys. Rev. B **74**, 144423 (2006); W. H. Zurek, U. Dorner, and P. Zoller, Phys. Rev. Lett. **95**, 105701 (2005); J. Dziarmaga, *ibid.* **95**, 245701 (2005).

<sup>3</sup>T. Caneva, R. Fazio, and G. E. Santoro, Phys. Rev. B **76**, 144427 (2007); F. Pellegrini, S. Montangero, G. E. Santoro, and R. Fazio, *ibid.* **77**, 140404(R) (2008); T. Caneva, R. Fazio, and G. E. Santoro, *ibid.* **78**, 104426 (2008).

<sup>4</sup>F. M. Cucchiatti, B. Damski, J. Dziarmaga, and W. H. Zurek, Phys. Rev. A **75**, 023603 (2007).

<sup>5</sup>A. Polkovnikov, Phys. Rev. A **68**, 033609 (2003).

<sup>6</sup>R. Schützhold, M. Uhlmann, Y. Xu, and U. R. Fischer, Phys. Rev. Lett. **97**, 200601 (2006).

<sup>7</sup>M. Greiner, O. Mandel, T. Esslinger, T. W. Hänsch, and I. Bloch, Nature (London) **415**, 39 (2002).

<sup>8</sup>M. Albiez, R. Gati, J. Fölling, S. Hunsmann, M. Cristiani, and M. K. Oberthaler, Phys. Rev. Lett. **95**, 010402 (2005).

<sup>9</sup>R. Gati and M. K. Oberthaler, J. Phys. B **40**, R61 (2007).

<sup>10</sup>Y. Shin, G.-B. Jo, M. Saba, T. A. Pasquini, W. Ketterle, and D. E. Pritchard, Phys. Rev. Lett. **95**, 170402 (2005).

<sup>11</sup>S. Fölling, S. Trotzky, P. Cheinet, M. Feld, R. Saers, A. Widera, T. Müller, and I. Bloch, Nature (London) **448**, 1029 (2007).

<sup>12</sup>P. Cheinet, S. Trotzky, M. Feld, U. Schnorrberger, M. Moreno-Cardoner, S. Fölling, and I. Bloch, Phys. Rev. Lett. **101**, 090404 (2008).

<sup>13</sup>A. N. Salgueiro, A. F. R. de Toledo Piza, G. B. Lemos, R. Drumond, M. C. Nemes, and M. Weidemüller, Eur. Phys. J. D **44**, 537 (2007).

<sup>14</sup>G. J. Milburn, J. Corney, E. M. Wright, and D. F. Walls, Phys. Rev. A **55**, 4318 (1997).

<sup>15</sup>A. P. Tonel, J. Links, and A. Foerster, J. Phys. A **38**, 1235 (2005).

<sup>16</sup>S. Raghavan, A. Smerzi, S. Fantoni, and S. R. Shenoy, Phys. Rev. A **59**, 620 (1999).

<sup>17</sup>S. Raghavan, A. Smerzi, and V. M. Kenkre, Phys. Rev. A **60**, R1787 (1999).

<sup>18</sup>G. Kalosakas, A. R. Bishop, and V. M. Kenkre, Phys. Rev. A **68**, 023602 (2003).

<sup>19</sup>G. Kalosakas, A. R. Bishop, and V. M. Kenkre, J. Phys. B **36**, 3233 (2003).

- <sup>20</sup>W. Wernsdorfer and R. Sessoli, *Science* **284**, 133 (1999).
- <sup>21</sup>W. Wernsdorfer, R. Sessoli, A. Caneschi, D. Gatteschi, and A. Cornia, *Europhys. Lett.* **50**, 552 (2000).
- <sup>22</sup>J. Johansson, M. H. S. Amin, A. J. Berkley, P. Bunyk, V. Choi, R. Harris, M. W. Johnson, T. M. Lanting, S. Lloyd, and G. Rose, *Phys. Rev. B* **80**, 012507 (2009).
- <sup>23</sup>A. Polkovnikov, S. Sachdev, and S. M. Girvin, *Phys. Rev. A* **66**, 053607 (2002); M. Jääskeläinen and P. Meystre, *ibid.* **71**, 043603 (2005); A. K. Tuchman, C. Orzel, A. Polkovnikov, and M. A. Kasevich, *ibid.* **74**, 051601(R) (2006).
- <sup>24</sup>J. C. Eilbeck, P. S. Lomdahl, and A. C. Scott, *Physica D* **16**, 318 (1985); V. M. Kenkre and D. K. Campbell, *Phys. Rev. B* **34**, 4959 (1986); A. Smerzi, S. Fantoni, S. Giovanazzi, and S. R. Shenoy, *Phys. Rev. Lett.* **79**, 4950 (1997).
- <sup>25</sup>L. D. Landau, *Phys. Z. Sowjetunion* **2**, 46 (1932); C. Zener, *Proc. R. Soc. London, Ser. A* **137**, 696 (1932).
- <sup>26</sup>S. Dürr, T. Volz, and G. Rempe, *Phys. Rev. A* **70**, 031601(R) (2004).
- <sup>27</sup>K. Smith-Mannschott, M. Chuchem, M. Hiller, T. Kottos, and D. Cohen, *Phys. Rev. Lett.* **102**, 230401 (2009).
- <sup>28</sup>D. Witthaut, E. M. Graefe, and H. J. Korsch, *Phys. Rev. A* **73**, 063609 (2006).